GT2024-127637

AN ADDITIVELY MANUFACTURED TWO-FLUID HEAT EXCHANGER DESIGNED WITH TOPOLOGY OPTIMIZATION TOOLS

Claudio Caruso
Baker Hughes
Florence, IT

Francesco Morante
Baker Hughes
Florence, IT

Giacomo Pampaloni
Baker Hughes
Florence, IT

Stefano Rossin
Baker Hughes
Florence, IT

Alessandro Canova
ToffeeX
London, UK

Nicola Casari
ToffeeX
London, UK

Thomas Rees
ToffeeX
London, UK

ABSTRACT

Heat exchangers are widely used in gas turbine plants for several purposes, with traditional designs including shell and tube or plate-fin coolers. Recent developments in additive manufacturing techniques such as laser powder bed fusion have led to interest in the use of alternative heat exchanger designs, such as those generated with topology optimization techniques. These design techniques can result in more efficient heat exchangers with complex internal structures which can only be manufactured using additive techniques. Nevertheless, manufacturing heat exchangers for gas turbine applications with additive techniques is not straightforward. Two of the primary difficulties in the use of laser powder bed fusion are the printing of materials with high thermal conductivity such as copper alloys as well as powder cleaning from any complex internal channels such as those which may be generated by topology optimization tools.

To investigate the feasibility of combining topology optimization techniques with additive manufacturing to design novel heat exchangers a proprietary topology optimization software is used to design an oil/air cooler with significantly reduced size and pressure drop compared to an equivalent one based on a conventional design. In a potential future application on oil circuits, this could consequently result in an optimization of the lubricant oil circuit components, for example pumps, piping, console dimensions and weight. The design was also optimized to consider manufacturability constraints such as overhang angles and minimum thickness as well as to correct in line with feedback from initial trial prints. The cooler was manufactured using additive manufacturing techniques.

Keywords: heat exchanger, cooler, topology optimization, additive manufacturing, biomimicry

NOMENCLATURE

AM	Additive Manufacturing
CFD	Computational Fluid Dynamics
CHT	Conjugate Heat Transfer
DfAM	Design for Additive Manufacturing
CAE	Computer Aided Engineering
CGM	Conjugate Gradient Method
EDM	Electro Discharge Machine
GD	Gradient Descent
HX	Heat Exchanger
L-PBF	Laser Powder Bed Fusion
MMA	Method of Moving Asymptotes
RANS	Reynolds-averaged Navier Stokes
Re	Reynolds number
TO	Topology Optimization
Ω	Design Domain
Γ	Design domain boundary
ρ	Fluid density
ω	Objective function weight
X	Generic Design variable
γ	Design variable
R_i	Optimization constraint
$\boldsymbol{u}$	Velocity
p	Pressure

P_0	Total Pressure
E	Thermal Energy
ν	Viscosity
ν_t	Turbulent viscosity
D	Diffusivity coefficient
$\hat{n}$	Normal unit vector
$d\Gamma$	Boundary surface element

1. INTRODUCTION

Two fluid heat exchangers are widely used in various industrial applications where efficient heat transfer is necessary for optimal performance, **(WILSON, 1996)**. Particularly in the context of gas turbine plants, a common use is to cool the mineral and/or synthetic oils which feed the bearings of the gas turbines as well as other driven equipment (such as compressors, gearboxes, and generators). Traditional designs for these types of heat exchangers are shell and tube oil-water coolers or oil-air coolers. These designs often include finned pipes and turbulators in the oil tubes to increase heat transfer, **(MIN, 2009)**.

In recent years, engineers and researchers have explored new heat exchanger designs and manufacturing methods to meet the demands for increased thermodynamic efficiency, reduced weight, size, and operating costs. In particular, the increased capabilities of metal additive manufacturing techniques such as laser powder bed fusion (L-PBF) coupled with design for additive manufacturing (DfAM) software tools and techniques have enabled the design and production of unconventional geometries that cannot be manufactured using traditional manufacturing processes, **(Sing, 2020)**.

The scope of this paper is to present a series of design, analysis, and manufacturing activities to design, using a proprietary topology optimization (TO) software, an oil-air cooler with significantly reduced size and total pressure drop in the oil circuit compared to an equivalent cooler design based on conventional approach and manufacturing techniques.

2. PREVIOUS WORK & BACKGROUND
2.1 TOPOLOGY OPTIMIZATION

The design software for the cooler presented in this paper is based on topology optimization (TO). TO is a mathematical optimization method which finds an optimal distribution of a scalar design variable γ in a domain Ω with boundaries Γ while simultaneously respecting a set of linear or nonlinear constraints $R_i = 0$, which are usually chosen to represent a set of physical governing equations for the problem [1]. Topology optimization problems are solved iteratively as an adjoint-based optimization problem (either discrete or continuous), with γ being updated with an optimization method such as gradient descent (GD) [2], or the method of moving asymptotes (MMA) [3].

One of topology optimization's major strengths is that it generates a (locally) optimal geometry starting from an empty design domain Ω. In other words, it calculates the optimal geometry 'from scratch' instead of modifying an existing geometry to improve its performance.

In industrial applications, TO is primarily used as a structural design tool for applications such as light weighting of structural members, for example: struts, brackets, or cantilevers [4]. Recent research has explored the concept of using TO for more complicated physical problems such as fluid dynamics [5] or electromagnetics [6]. These are far more challenging optimization problems due to the nonlinearity of their governing equations (in the case of the Navier-Stokes equations for fluid dynamics) or the number of state variables and governing equations (Maxwell's equations for electromagnetics). In order to optimize for realistic flow conditions, the Reynolds averaged Navier-Stokes (RANS) equations are used throughout this paper. As a result, turbulence is modelled using a two-equation eddy viscosity model, modified to account for the presence of solid in the optimization domain.

TO Techniques for optimizing two-fluid heat exchanger designs is a particular challenge [8] [9]. To develop a TO problem statement for two fluid heat exchangers an extra constraint must be imposed on the optimization problem (i.e. in addition to the governing equations) to ensure that the two fluids involved in the problem statement stay separate and do not mix.

Previous work [8] [9] has achieved this by using a single design variable $\gamma \in [0,1]$ for the two fluid problem. Generally, $\gamma = 0$ represents a region occupied by the first fluid and $\gamma = 1$ a region occupied by the second. Solid regions are represented by intermediate values of γ. The secondary design variables α_1 and α_2 can be calculated from the value of γ, where the exact relationship often needs to be adapted to work best with the specific optimization problem being considered. These latter two secondary design variables represent a Brinkmann-style impermeability which is used to represent the presence of a solid material in the optimization domain [5].

In summary, the two fluid heat transfer TO problem's objective function can be stated as follows:

$$\min_{\gamma} F(\boldsymbol{X}, \gamma) = \omega_1 \int_{\Gamma} P_{01} \boldsymbol{u_1} \cdot \hat{\boldsymbol{n}} d\Gamma +$$

$$\omega_2 \int_{\Gamma} P_{02} \boldsymbol{u_2} \cdot \hat{\boldsymbol{n}} d\Gamma + \omega_3 \int_{\Gamma} E\boldsymbol{u} \cdot \hat{\boldsymbol{n}} d\Gamma \tag{1}$$

The objective function must be optimized subject to the following constraints:

$$R_{p_1} = \nabla \cdot \boldsymbol{u_1} = 0 \tag{2}$$

$$R_{p_2} = \nabla \cdot \boldsymbol{u_2} = 0 \tag{3}$$

$$R_{\boldsymbol{u_1}} = \boldsymbol{u_1} \cdot \nabla \boldsymbol{u_1} + \frac{\nabla p_1}{\rho_1} - (\nu_1 + \nu_{t1})\nabla^2 \boldsymbol{u_1} + \alpha_1(\gamma)\boldsymbol{u_1} = 0 \tag{4}$$

$$R_{\boldsymbol{u_2}} = \boldsymbol{u_2} \cdot \nabla \boldsymbol{u_2} + \frac{\nabla p_2}{\rho_2} - (\nu_2 + \nu_{t2})\nabla^2 \boldsymbol{u_2} + \alpha_2(\gamma)\boldsymbol{u_2} = 0 \tag{5}$$

$$R_E = (\boldsymbol{u_1} + \boldsymbol{u_2}) \cdot \nabla E - \nabla \cdot (D\nabla E) = 0 \tag{6}$$

The multi-objective function, described in eq. (1),is a weighted sum of individual terms representing 1) total pressure losses in the first fluid, 2) total pressure losses in the second fluid and 3) thermal energy transfer to/from the first fluid. Assuming adiabatic walls, the last term in the objective function represents the heat duty of the entire heat exchanger. This objective function is minimized subject to the following constraints:

2

The latter equation represents a 'unified' energy equation for the system. The Brinkmann terms in the governing momentum equations, (4) and (5),ensure that the individual fluid velocities u_1 and u_2 are numerically insignificant in both the solid regions of the domain and in the complementary fluid region. Therefore, the unified energy equation, (6),essentially reduces to a steady-state heat diffusion equation in the solid region, and the relevant advection-diffusion equation in each fluid region. As we consider the incompressible Navier-Stokes equations, the incompressibility condition is expressed by eq (2) and (3).

The constraints must also include an appropriate set of boundary conditions for the governing equations. These are briefly summarized as follows:

At inlets: Dirichlet conditions on temperature and velocity. Neumann condition on pressure

At outlets: Dirichlet conditions on pressure. Neumann conditions on velocity and temperature.

At walls: Dirichlet (no-slip conditions) on velocity. Neumann conditions on pressure and temperature (adiabatic wall conditions).

2.2 PHYSICS DRIVEN GENERATIVE DESIGN TOOL

The two fluid heat exchanger designs presented in this paper were generated using a proprietary physics-driven design computer aided engineering (CAE) software tool developed by ToffeeX Ltd. Based primarily on TO methods such as those described in the previous section, the software uses a finite volume method Reynolds-averaged Navier Stokes (RANS) solver to solve the governing equations based on user-defined boundary conditions. The solid field is represented in the fluid TO problem with a Brinkmann impermeability term, however, both the optimization solver as well as the precise TO model are proprietary.

In addition to providing the boundary conditions and the design domain for the topology optimization problem, uses of the software must provide information about the fluid(s) and solid material(s) to be used in the TO simulation. Users can also specify global and local geometry constraints and physics effects based on the specific requirements of the design (see Section 3).

2.3 POWDER BED FUSION ADDITIVE MANUFACTURING

Additive Manufacturing (AM) technologies include lots of different techniques. The common principle is that the construction of the object achieved by material addition instead of removal and it usually occurs layer by layer, **(F. Calignano et al., 2017)**. The selection of the best AM technology for each application is a tradeoff between size and resolution. Small printers usually allow very high resolution and material quality. On the other hand, big machines cannot guarantee accuracy while printing small features.

For this work, Laser Powder Bed Fusion (L-PBF) technology was selected. This is one of the most commonly used AM methods to realize complex metal parts. It allows the printing of fully dense material (>99,9%) with high resolution. The process uses a laser source to melt base material that is in the form of fine metal powder. The bigger systems on the market can provide a building volume of around one cubic meter with several lasers that work together to increase productivity. Few machines on the market are also able to print high-conductivity materials such as copper alloy.

One of the main limitations of L-PBF is the impossibility to print features with high overhang angle with respect to the build platform. This restriction imposes some constraints that must be implemented during the component design phase. Other limits while printing large parts (i.e. >100mm) are shrinkages and deformations. It's possible to compensate for those behaviors using simulations and iterative procedures.

3. DESIGN PROCESS AND RESULTS

Physics-driven generative design engineering tools provide engineers with the capability of rapidly generating designs and iterating through them during the design process. To illustrate the rapid iteration process, this section presents a subset of design iterations generated with the software described in Section 2. Throughout this iterative process, the design and simulation problems submitted to the software were changed based on several considerations, not only from the perspective of the heat exchanger's performance but also based on the requirements for manufacturing and testing.

3.1 INITIAL TEST CASE STUDIES

The initial design cycles for the heat exchanger were based on simple proof-of-concept problems to illustrate if the generative design technology could produce practically useful designs, i.e. designs which are effective both from a heat transfer perspective as well as being manufacturable using powder bed fusion techniques. At this stage of the design process, no specific consideration was given to the actual performance of the generated geometries or even to ensuring the properties of the fluids and solid materials used would match those of the final design problem. Instead, a successful outcome was one which was judged to be manufacturable with L-PBF with minimal pre- or post-processing, and whose design made engineering sense (intuitively) to achieve heat exchange at a minimal total pressure loss.

The test case chosen for this purpose is a cross-flow designed heat exchanger unit. The design domain submitted to the design software is shown in Figure 1a. It is a half-cube design domain with a single inlet and outlet for each fluid arranged in

crossflow. The Reynolds number at the inlets for each fluid was set to Re = 100. The material chosen was stainless steel.

Figure 1 shows the results obtained when the design algorithm was run in an unconstrained formulation. The software generates a geometry which consists of a solid stainless steel "membrane" which separates the hot and cold fluids. The membrane creates tortuous fluid paths, increasing the effective heat transfer surface area and consequently the heat transfer coefficient.

Figure 2 shows the results for the same simulation with an active overhang constraint. This is a geometric constraint on the design variable which minimizes the regions of overhanging solid beyond a certain overhang angle (set to 45 degrees for this application). Although the generated geometry still has some regions of overhang, they are significantly minimized while also maintaining a similar high heat transfer surface area design as the unconstrained design.

Based on these results, the software tool's two-fluid heat exchanger design methodology was found to be effective enough to move to a more detailed design process.
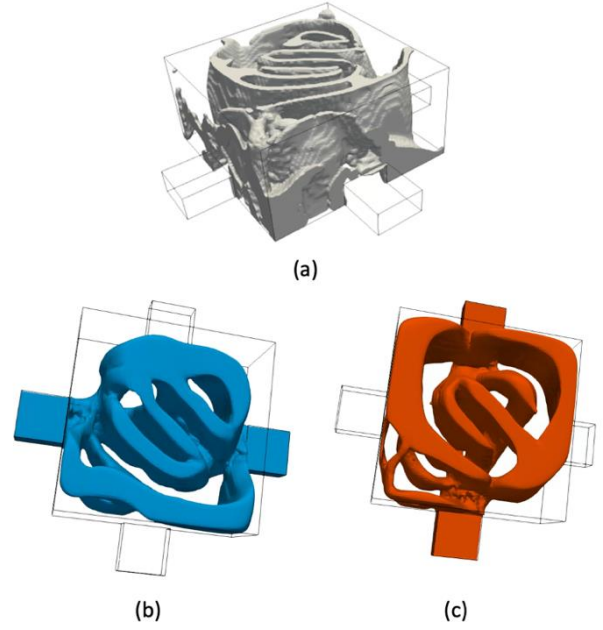

Figure 2: Results of a design simulation with a constraint on the solid overhang angle. (a) shows the solid part separating the two fluids, while (b) and (c) show the cold-side and hot side fluid domains respectively.

Figure 1: Results of a design simulation for a two-fluid heat exchanger. (a) shows the design domain, (b) shows the two fluid domains (in red and blue) and the solid part (in grey). (c) shows the cold side fluid domain. (d) shows the hot side fluid domain. (e) shows the solid part separating the two fluids.

3.2 HEAT EXCHANGER DESIGN CHOICES

The first design iterations for realistic operating conditions were based on the concept of building a heat exchanger from a replicated periodic unit cell. In this case, periodic boundary conditions are enforced on the flow fields, and as a result, the geometry has the same periodic structure. The velocity profiles are equal on each pair of periodic surfaces, and therefore, the flow field will approximate the flow field in a single unit of the heat exchanger core. The pressure drop across the full heat exchanger can be approximated by multiplying the pressure drop over a single unit by the number of units in the flow direction.

The approach of using a lattice of periodic unit cells has already been proven as an effective DfAM solution for heat exchangers. These structures resemble the ones present in nature such as butterfly wings, and cell membranes, (D.G) (Deng). Previous efforts have primarily used gyroid-type unit cells, which can be generated using several DfAM software tools.

Using the software's periodic boundary condition functionality, a periodic unit cell can be generated based on a fluid topology optimization problem. This approach has several advantages for achieving the design requirements. Firstly, it significantly reduces the computational cost of the topology optimization problem as only a very small subset of the entire heat exchanger geometry needs to be simulated and designed. Secondly, by building a heat exchanger with a modular design, the engineer is assured that the complete

4

heat exchanger will satisfy all the requirements that the individual module (or unit cell) satisfies. For example, in the context of manufacturability, if it is known that a single periodic unit cell module can be manufactured using a specific technique then it is likely that the entire heat exchanger can be manufactured.

However, despite the significant advantages, the periodic unit cell lattice technique has also several drawbacks:

Variations across the heat exchanger: Unit cell geometries are uniform across the heat exchanger and are therefore not optimized to account for variations in system properties across the entire heat exchanger, in particular fluid temperatures and velocities. For example, some regions of the heat exchanger will have higher temperature differences between the hot and cold fluids, resulting in a higher heat transfer in these regions compared to others. The periodic design approach cannot optimize geometries to take advantage of these large-scale variations. Furthermore, the flow through the real heat exchanger will never be completely periodic, which is the central assumption in the design algorithm. This will likely lead to sub-optimal designs.

Integration with other components: The periodic unit cell approach to heat exchanger design (by definition) only generates an optimized geometry for a single cell – other, critical aspects of the cooler design such as inlet or outlet manifolds must be considered in a separate design process. With a monolithic design approach (described below), the whole optimization problem (including inlet and outlet manifolds) for the entire component can be specified. This means that the optimization problem can be defined at the outset, leading to the optimization of the entire heat exchanger system in a single process.

Performance prediction of full-scale component: Finally, when generating a single periodic unit cell, the output from the generative design software only gives information about the performance of a single periodic cell under the assumptions of a fully periodic problem with a fixed temperature difference between the two fluids. In order to then calculate or predict the performance of the entire heat exchanger (which may contain thousands, or in some cases tens of thousands of these unit cells) a separate calculation needs to be made. Due to the multiscale nature of this problem, calculating the performance of the full-scale component using a high-fidelity physics simulation like conjugate heat transfer CFD simulations is extremely computationally expensive due to the large mesh size. Consequently, any prediction of the performance of the full-scale design will often require the development of a reduced-order engineering model, whose performance predictions will be less accurate than a full-scale simulation.

3.3 PERIODIC UNIT CELL HEAT EXCHANGER

To investigate the periodic unit cell approach, a periodic design domain of a cube of 3 cm size was used to run a series of periodic fluid topology optimizations, maintaining the same volumetric flow rates through both fluid systems and increasing the heat transfer objective weighting. The results are shown in Figure 3. Different optimization solution attractors manifest as the objective function is increased. Figure 3(b) shows a solution consisting of flat plates separating the hot and the cold fluids in alternating manners, Figure 3(c) shows a solution based on tubes containing one of the fluids, while the other flows around, Figure 3(d) shows a more complex solution reminiscent of gyroid type geometries (although not a gyroid geometry itself), while Figure 3(e) shows a geometry with a high level of complexity. Each of these geometries shows increasing levels of complexity, resulting in higher pressure losses across the two fluid systems (but also higher heat transfers).

Based on this initial study, several more TO design iterations resulted in the generation of an initial geometry for more detailed analysis (Figure 4(a)). This geometry showed a high degree of complexity and heat transfer surface area while also indicating acceptably low pressure losses across the system (especially compared to the geometry presented in Figure 3(e)).

To have a more accurate understanding of the performance of this geometry, a high-fidelity conjugate heat transfer CFD simulation was performed on a 4x4x4 lattice (Figure 5(a)) of this unit cell. Based on the high-fidelity conjugate heat transfer simulation performed (and through extrapolation of the results), the desired heat transfer would have been obtained using a 12x12x4 lattice of unit cells (Figure 4(b)).
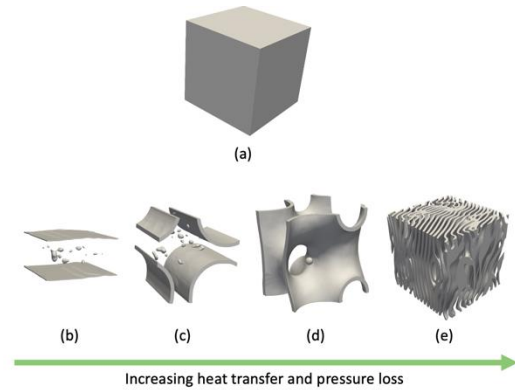

Figure 3: Two fluid heat exchanger design results for a periodic unit cell. (a) shows the design domain, and (b) to (e) the results of optimization processes with different relative weightings between pressure losses and heat transfer.
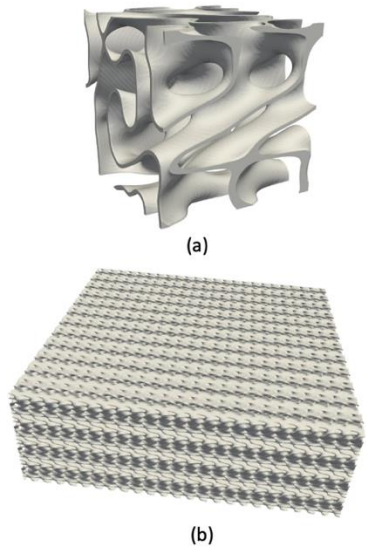
(a)

(b)

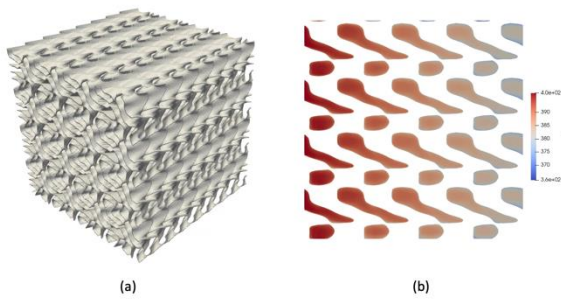*Figure 4: The final periodic unit cell design (a) with a 12x12x4 lattice built from the unit cell (b)*

(a)

(b)

Figure 6: Conjugate Heat transfer CFD results from a 4x4x4 lattice of the unit cell.

3.4 MONOLITHIC HEAT EXCHANGER DESIGN

Following the design exercise for the periodic unit cell lattice-based heat exchanger solution, a second design approach was investigated. This approach involved a quasi-monolithic topology optimization which modelled the physics throughout the entire cooler rather than a single triply periodic unit cell. As discussed in Section 3.2, in order to achieve a similar level of fidelity to the periodic unit cell optimization, a much higher resolution computational mesh is required. This results in a much higher computational cost for the optimization process. Furthermore, a much higher resolution mesh introduces significantly more degrees of freedom to the topology optimization process, which can introduce many more locally optimal solutions.

By simulating the entire heat exchanger, the software's optimization process accounts for temperature and velocity variations across the entire heat exchanger, ensuring that the highest heat transfer (and associated pressure losses) occurs in regions of the domain where these mechanisms are most effective. The trade-off is the reduced geometry complexity caused by the coarser computational mesh.

3.4.1 FIRST ITERATION

The first design iteration using the generative design software for a monolithic heat exchanger design was performed using the design domain presented in Figure 6a. The oil side and air side are arranged in crossflow, with the oil being fed into the cooler through an array of pipes, while the air is passed through a large duct. Notably, the design domain is not a true 'monolithic' design domain; it is divided into four layers or slices stacked in the transverse direction. The optimization algorithm is then run on a single slice with symmetry boundary conditions in the 'slice' direction.

The decision to simplify the design of the heat exchanger in this way was based on two justifications. Firstly, performing a simulation on the entire heat exchanger was computationally prohibitively expensive to effectively run rapid design iterations on the geometry (the mesh size would have been order 10^7 cells). Secondly, with a heat exchanger arranged in the crossflow configuration, the simplification of dividing the domain into slices along the transverse direction still captures the important variations of fluid temperatures across the domain (overcoming one of the primary drawbacks of the periodic design), and so, the design algorithm can capture them and include them in its optimization calculations. The size of the design domain is 360x360x300 mm, giving a total cooler size of when the slices are stacked on one another.

Figure 7 shows the geometry generated during the first design iteration. No geometrical constraints were specified on the design at the stage. The results show an extremely complex geometry reminiscent of biological structures. Based on the outcomes of the first design iteration, some improvements were identified:

- The oil inlet/outlet structure (24 pipes each) was very complex and difficult to manufacture/introduced a larger number of failure points.
- The design domain resulted in a HX which was slightly too large to fit in a single AM machine and needed to be reduced.
- Strict manufacturing (overhang) constraints need to be applied to the design simulation. The unconstrained design results were far too far away from a manufacturable solution to allow a manual postprocessing fix.
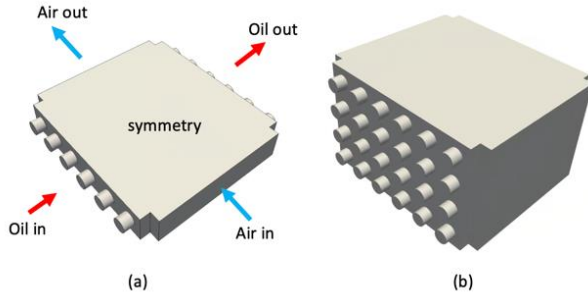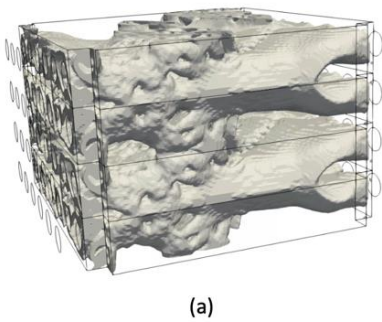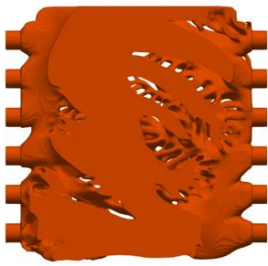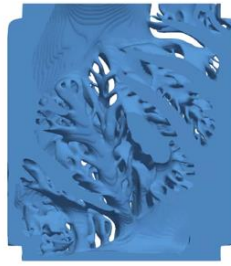
Figure 6:(a) shows the design domain for the first iteration of the monolithic heat exchanger (b) shows the arrangement of design domains to create the full-scale heat exchanger core.


Figure 7: Design simulation results for the first iteration of the monolithic heat exchanger design. (a) shows the solid part/membrane (b) the hot side fluid and (c) the cold side fluid

3.4.2 SECOND ITERATION

Following the first design iteration for the monolithic heat exchanger design approach, a second design was generated with four modifications to the design problem statement. First, a new domain was generated for the optimization process. The new domain is smaller in size, ensuring printability on the selected AM machine. It includes simpler manifold/inlet/outlet regions to reduce the complexity associated with designing inlet and outlet manifolds. The new layout also arranges the oil inlet and outlet on the same side of the heat exchanger to comply with requirements of the experimental test apparatus. In addition, walls on each slice have been added to ensure the manufacturability of the final geometry by introducing extra supporting structures.

Second, the design optimization simulation was carried out with geometric overhang constraints imposed on the optimization process. Third, the overall geometry was divided into five regions. This choice was made as a compromise between the computational cost of the topology optimization simulations and the level of detail desired in the final optimized geometry. Reducing the size of the design domain allowed for a coarser mesh allowing for more rapid design simulation. Finally, a minimum wall thickness constraint of 1.5 mm was imposed on the design. Although much larger than the minimum printable feature size of the machine used to manufacture the part, this conservative value was chosen to ensure complete water tightness of the two fluid regions. Such a large wall thickness will inevitably result in lower performance of the cooler as it will both decrease the heat transfer as well as increase the blockage effect (and thus pressure losses) for both hot and cold side. Further design iterations and manufacturing tests would need to be performed to confirm the minimum wall thickness for the design which would be reliably manufacturable to an acceptable quality.

The output of the second design iteration loop is shown in Figure 8. When compared to the first iteration's geometry output the geometry is significantly less complex, with larger channels and much thicker walls.
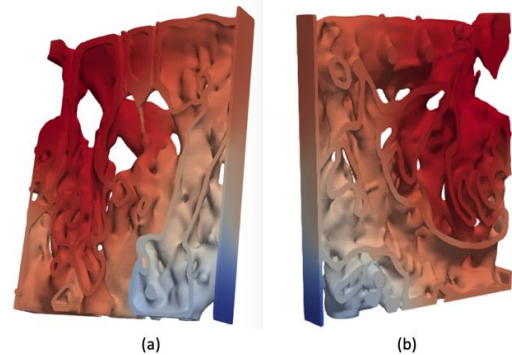
Figure 8: Temperature profile on core design for the second iteration of the monolithic heat exchange design. Note the simpler geometry and thicker walls.
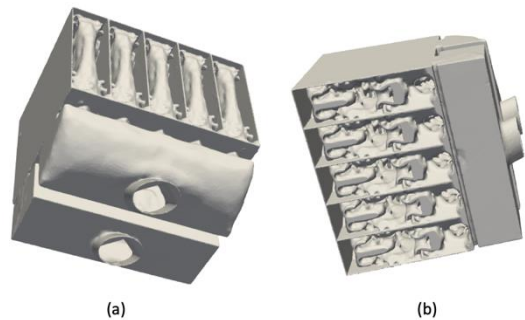
Figure 9: The final, complete design of the integrated heat exchanger, including core layers designed using the monolithic approach as well as the integrated manifolds.

3.5 INLET AND OUTLET MANIFOLDS AND INTEGRATION

To complete the design and make it ready for manufacture and test, the same topology optimization software was used to perform a detailed design of the oil inlet and outlet manifold connectors independently from the heat exchanger core design. In the case of the outlet manifold design, this is a relatively trivial process where the outlets from the heat exchanger core need to be directed to a single outlet pipe while minimizing any pressure losses – this requires a single fluid pressure loss topology optimization solution. The result is shown in Figure 10.
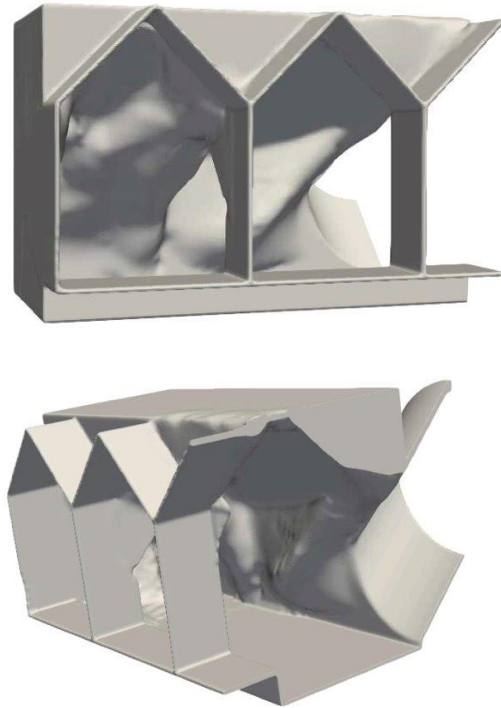

Figure 10 – Outlet manifold

The inlet manifold design is slightly more complex as it needs to evenly split the incoming oil flow and distribute it to the five separate core regions while also minimizing any pressure losses. This is complicated by the relatively narrow oil feed pipe inlet diameter (3 inch) and the very large inlet areas for each of the core slices. The oil flow therefore needs to go through a strong expansion region (negative pressure gradient) which is likely to cause flow separation and recirculation – contrary to the pressure loss minimization objective function.

The topology optimization objective function used to generate the inlet manifold is defined to match a specified velocity vector distribution in a domain and generates the design to guarantee such target is achieved. This functionality can be applied both to regions inside the domain or at surfaces on the boundary. With respect to this geometry, the target domains are placed close to the boundary, and in each target, a velocity vector is prescribed to be equal to one-fifth of the inlet flow rate. In this way, each of the five regions receives the same flow rate whose sum is the inlet flow rate. In addition, the symmetry of the domain is exploited and only half of the inlet manifold is considered.

The starting domain is reported in Figure 11 with highlighted the regions to which the velocity target is applied highlighted. The problem is setup by applying the flow rate at the inlet and using a zero-pressure outlet boundary condition.
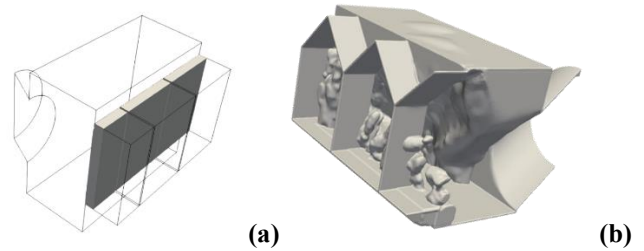

(a)   **(b)**

Figure 11 – a) Computational domain for the inlet manifold with the highlighted region where the velocity target is applied - b) Final shape of the inlet manifold domain.

The inlet manifold final geometry is reported in Figure 11 (b). It can be clearly seen how the TO tries to block the stream of oil which would naturally go in the central module as it is placed directly in front of the inlet. The blockage created by the solidity blocks displaced in the central "window" causes a large-scale vortex which develops in the width of the manifold and that is deflected inside each of the modules by airfoil-like structures in the other two windows. This ensures the flow is deflected inside the module uniformly. It is crucial to remark here that the overhang constraint has been enforced during the optimization. This is clearly visible by looking at the internal structures and at the "roof" of the windows that has been generated at 45°. The lower base on the other hand is not overhang compliant as supports can be added there and they don't interact with the flow field.

The outputs from each of the optimization simulations described above are STL surface mesh files, which need to be merged into a single geometry file ready for printing. The final geometry for printing is rendered in Figure 9.

4. PERFORMANCE COMPARISONS TO CONVENTIONAL DESIGNS

The performance (measured in terms of total heat duty and both oil- and air-side pressure losses) of the monolithic heat exchanger design was calculated using conjugate heat transfer CFD simulations using steady-state RANS equations to solve the fluid flow problem. To simplify and reduce the computational cost of the CFD problem, instead of meshing and simulating the entire geometry (as shown in Figure 9), only a single slice of the heat exchanger core was meshed and simulated. The full-scale

heat exchanger performance was then extrapolated from the performance of the single slice.

Conjugate heat transfer is a technique that allows to extract the effective heat transfer by solving the energy equation across the whole domain, i.e. the two fluids and the solid. In order to do this, the advection-diffusion equation is solved in the fluid regions, while in the solid it reduces to a heat equation.

The performance of the cooler designed in Section 3 is compared to a simplified design of a finned air cooler obtained by a traditional design tool (HTRI), while imposing equivalent size and thermodynamic design data (het duty, flowrates, fluids inlet temperature).

The conventional cooler design achieves a total heat duty of approximately 14kW with an oil side pressure drop of 1.2 bar, comparing favorably to the topology optimization designed cooler which achieves approximately the same heat duty with an order of magnitude decrease in the oil-side pressure drop (pressure drop lower than 0.1bar estimated for the core). Pressure drops on the air side are comparable between the two designs.

The significant differences in the oil side pressure drop are due to the significantly different oil-side velocities during the two coolers. In the case of the finned air cooler, the oil needs to be pumped through 5/8" external diameter tubes which themselves are filled with turbulators which further increase the blockage effect and pressure losses across the system.

In contrast, the TO heat exchanger uses a much larger average cross-sectional area through the oil side area, resulting in an oil side velocity on the order of 1e-3 m/s, and consequently a much lower total pressure loss. A recap of the comparison is represented in the table below.

	TO printed cooler	Traditional HX
Design	Topology Optimization SW	HTRI
Internal Layout	Internal path optimized by TO software	96 finned 5/8" pipes with turbulators, reduced pitch
Dimension	400 x 400 x 350 mm overall (core + in/out connection)	Pipe length 400mm 300 mm longitudinal
Heat duty	14 kW	
Oil flowrate	60 l/min	
Air flowrate	2000 m3/h	
Oil side pressure loss (estimated)	2000 Pa (0.02 bar)	1.2 bar
Air side pressure loss (estimated)	1000 Pa	990 Pa

Table 1: Comparison of TO optimized cooler vs traditional design.

5. MANUFACTURING

The heat exchanger prototype was printed by Baker Hughes on an EOS® M400 powder bed fusion system (build volume 400 x 400 x 400 mm). The layers were exposed with a hatching and contour scan strategy. The main aim of this printing was to demonstrate the ability of the system to produce large complex parts. A build interruption was necessary to refill the metal powder inside the system, change machine filter and clean

overflow bin. This made it possible to print the entire part in one single job.

After the print, the part was detached by the build platform, by means of Electro Discharge Machine (EDM) cut and divided into 6 slices to perform measurements of the internal channels. Figure 12 below shows one of the slices after surface treatment. Separation from the building platform caused a significant material loss due to part shrinkage (Figure 13).

Figure 12 Example of topology optimized part section

Figure 13: Comparison between 3D model and printed part

A light scan technique was used to measure the magnitude of surface deviations from the theoretical model (Figure 14). This information will be used to compensate any following prints. The main misalignment highlighted by the measure was a discontinuity inside the component caused by the build interruption. Although it was visible to the naked eye, the light scan made it possible to clearly map the magnitude of this issue in the component. Wall thickness in some critical areas was also measured, relying on light scan results (Figure 15).
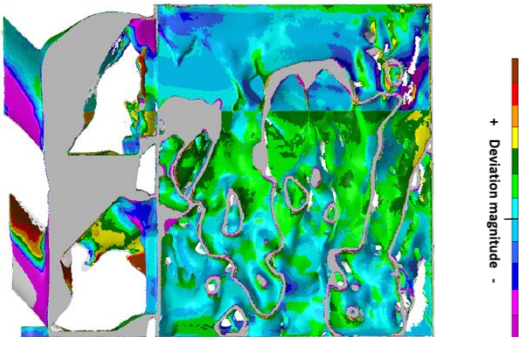

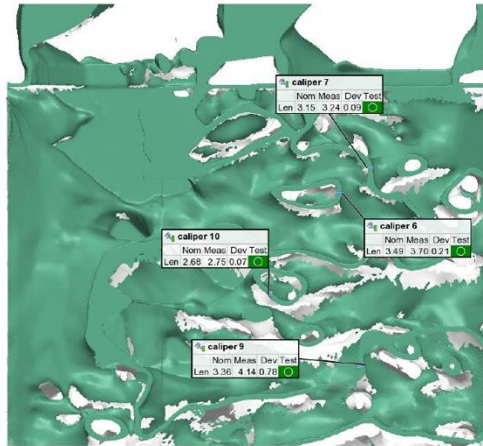Figure 14 - Light scan measure results on topology optimized part's slice

Figure 15 - Comparison between nominal and real wall thickness.

6. CONCLUSIONS AND NEXT STEPS

The activities presented in this paper confirm the high potential benefit of using topology optimization techniques with additive manufacturing for the design of efficient and compact heat exchangers. While the major gain at the moment is seen in the fluid pressure drop reduction, potential space is foreseen also on additional size reduction, taking also into account some learning from the completed activities.

In particular the following lessons have been learned on the TO design iteration process:

- Generally, manufacturability can be satisfied using the techniques available, however, the required constraints need to be established at the outset – it may take a lot of time/many iterations to generate satisfactory designs.
- In general, periodic optimization approaches provide better performance/more compact heat exchangers.
- Improvements in optimization algorithms are necessary to better explore the Pareto front of the optimization problem. The manufactured design has significant oil-side pressure loss overhead which can be used to achieve a higher heat transfer and additionally improve performance.

Similarly, some Lessons learned were identified from the manufacturing process:

- Base material needs to be increased to avoid thickness reduction due to part shrinkage.
- Job interruptions can cause part misalignments and associated print quality failures.
- Remove bulk material area to reduce printing time and cost.
- Reduce wall thickness to increase heat exchange value.

Follow on work will include a second print trial of the heat exchanger along with experimental testing.

REFERENCES

[1] M. P. Bendsoe and O. Sigmund, Topology optimization: theory, methods, and applications, Springer Science \& Business Media, 2003.

[2] M. Pietropaoli, F. Montomoli and A. Gaymann, "Three-dimensional fluid topology optimization for heat transfer," *Structural and Multidisciplinary Optimization,* vol. 59, no. 1, pp. 801-812, 2019.

[3] K. Svanberg, "The method of moving asymptotes—a new method for structural optimization," *International journal for numerical methods in engineering,* vol. 24, no. 2, pp. 359-373, 1987.

[4] A. L. R. Prathyusha and G. Raghu Babu, "A review on additive manufacturing and topology optimization process for weight reduction studies in various industrial applications," *Materials Today: Proceedings,* vol. 62, no. 1, pp. 109-117, 2022.

[5] J. Alexandersen and C. S. Andreasen, "A review of topology optimisation for fluid-based problems," *Fluids,* vol. 29, no. 1, p. 29, 2020.

[6] P. Bettini, P. Alotto, V. Cirimele, R. Torchi and F. Lucchini, "Topology Optimization for Electromagnetics: A Survey," *IEEE Access,* vol. 10, no. 1, pp. 98593-98611, 2022.

[7] C. Lundgaard, J. Alexandersen, M. Zhou, C. S. Andreasen and O. Sigmund, "Revisiting density-based topology optimization for fluid-structure-interaction problems," *Structural and Multidisciplinary Optimization,* vol. 58, no. 1, pp. 969-995, 2018.

[8] L. C. Høghøj, D. R. Nørhave, J. Alexandersen, O. Sigmund and C. S. Andreasen, "Topology optimization of two fluid heat exchangers," *International Journal of Heat and Mass Transfer,* vol. 163, no. 1, 2020.

[9] H. Kobayashi, K. Yaji, S. Yamasaki and K. Fujita, "Topology design of two-fluid heat exchanger," *Structural and Multidisciplinary Optimization,* vol. 63, no. 2, pp. 821-834, 2021.